Published in final edited form as:
Free Radic Biol Med. 2012 July 15; 53(2): 194–207. doi:10.1016/j.freeradbiomed.2012.04.005.

Cardiac Overexpression of Metallothionein Rescues Cold Exposure-Induced Myocardial Contractile Dysfunction through Attenuation of Cardiac Fibrosis Despite Cardiomyocyte Mechanical Anomalies

Yingmei Zhang[1,2,*], **Nan Hu**[2,*], **Yinan Hua**[2,*], **Kacy L. Richmond**[2], **Feng Dong**[2], and **Jun Ren**[2]

[1]Department of Cardiology, Xijing Hospital, Fourth Military Medical University, Xi'an, China 710032

[2]Center for Cardiovascular Research and Alternative Medicine, University of Wyoming College of Health Sciences, Laramie, WY 82071, USA

Abstract

Cold exposure is associated with an increased prevalence for cardiovascular disease although the mechanism is unknown. Metallothionein, a heavy metal scavenging antioxidant, protects against cardiac anomalies. This study was designed to examine the impact of metallothionein on cold exposure-induced myocardial dysfunction, intracellular Ca^{2+} derangement, fibrosis, ER stress and apoptosis. Echocardiographic, cardiomyocyte function and Masson trichrome staining were evaluated in friendly virus B (FVB) and cardiac-specific metallothionein transgenic mice following cold exposure (3 mo, 4°C). Cold exposure increased plasma levels of norepinephrine, endothelin-1 and TGF-β, reduced plasma NO levels and cardiac antioxidant capacity, enlarged ventricular end systolic diameter, compromised fractional shortening, promoted ROS production and apoptosis, and suppressed ER stress marker Bip, calregulin and phospho-eIF2α accompanied with cardiac fibrosis and elevated levels of matrix metalloproteinases and Smad-2/3 in FVB mice. Cold exposure-induced echocardiographic, histological, ER stress, ROS, apoptotic and fibrotic signaling changes (but not plasma markers) were greatly improved by metallothionein. *In vitro* metallothionein induction by zinc chloride ablated H_2O_2- but not TGF-β-induced cell proliferation in fibroblasts. In summary, our data suggested that metallothionein protects against cold exposure-induced cardiac anomalies possibly through attenuation of myocardial fibrosis.

Keywords

Cold exposure; Metallothionein; Contraction; ROS; Fibrosis; Apoptosis

Correspondence should be addressed to: Dr. Jun Ren, Professor University of Wyoming College of Health Sciences, Laramie, WY 82071, USA; Tel: (307)-766-6131; Fax: (307)-766-2953; jren@uwyo.edu.
*Equal Contribution

DISCLOSURES None.

INTRODUCTION

Extremely cold weather is associated with overtly increased cardiovascular morbidity and mortality [1–4]. A study performed in Czech Republic over a 21-year period from 1986 to 2006 reported that cold temperature is positively correlated with the cardiovascular mortality in all age groups for both genders [5, 6]. In particular, exposure to cold temperature has been demonstrated to precipitate angina pectoris in approximately 40% of patients with symptomatic coronary artery diseases [7–9]. The sequelae of cold exposure on health are more pronounced in individuals with cardiovascular and respiratory illness [8]. Recent data demonstrated that a 10°C drop in ambient air temperature may be associated with a 13% rise in coronary event, an 11% rise in incident and coronary death, and a 26% increase in recurrent event [10]. These findings prompt the notion of cold stress as an independent potential risk factor for cardiovascular diseases. Nonetheless, the precise mechanisms responsible for cold exposure-induced myocardial anomalies remain poorly understood. Recent finding revealed a compensatory increase in the antioxidant defense enzymes following long-term cold exposure possibly depicting a role of elevated reactive oxygen species (ROS) in low ambient temperature-associated health problems [11]. However, whether oxidative damage is the ultimate culprit factor in cold exposure-induced organ failure is still controversial as no conclusive evidence is available with regards to the effect of antioxidant in cold exposure. To this end, the present study was designed to examine the effect of metallothionein, a low molecular weight heavy metal chelating antioxidant, on chronic cold exposure-induced cardiac remodeling and contractile dysfunction, if any. Recent evidence from our lab and others has indicated pivotal cardioprotective properties of metallothionein against diabetes, obesity, insulin resistance, aging and hypertension-induced cardiac morphological and functional anomalies [12–18]. In particular, metallothionein has been shown to counteract cardiac fibrosis under stress conditions such as diabetes and nicotine exposure [17, 19]. Echocardiographic, cardiomyocyte contractile and intracellular Ca^{2+} properties, cardiac fibrosis, ROS accumulation, myocardial antioxidant defense including Cu Zn-superoxide dismutase (SOD1), catalase and glutathione, apoptosis as well as plasma levels of norepinephrine, endothelin-1 (ET-1) and nitric oxide (NO) were evaluated in adult wild-type friendly virus B (FVB) and cardiac-specific metallothionein overexpression transgenic mice following sustained cold exposure. Given that endoplasmic reticulum (ER) stress, hypoxia inducible factor (HIF-1α), angiotensin II and NO cascades have been implicated in cold stress [20–22], essential protein markers of ER stress [Bip, Calregulin, CHOP, eukaryotic initiation factor 2α (eIF2α) and inositol-requiring protein-1α (IRE1α)], HIF-1α, angiotensin II AT_1 receptor and endothelial NO synthase (eNOS) were also monitored in myocardium of metallothionein transgenic and FVB mice with or without cold exposure. To better understand the machinery of cardiac remodeling in particular fibrosis, the prominent forms of matrix metalloproteinases (MMPs) involved in the extracellular matrix formation namely MMP-2 and MMP-9 [23, 24], were scrutinized in the hearts from FVB and metallothionein mice with or without cold exposure. Given the critical roles of transforming growth factor β (TGF-β) and the Smad transcription factor, the key molecule for the initiation of TGF-β-mediated fibrosis, in extracellular matrix formation, interstitial fibrosis and tissue repair [25–29], levels of TGF-β and Smad-2/3 were examined in hearts from FVB and metallothionein mice with or without cold exposure.

MATERIALS AND METHODS

Metallothionein transgenic mice and chronic low temperature exposure

All animal procedures were approved by the Institutional Animal Care and Use Committee at the University of Wyoming (Laramie, WY, USA). In brief, transgenic mice with cardiac-specific overexpression of metallothionein (driven by the mouse α-MHC promoter) were described in detail previously [18, 30]. Three month-old male metallothionein transgenic

mice and their wild-type FVB littermates were housed at room temperature or low ambient temperature in a cold room (4°C) for 3 months [31] within the School of Pharmacy Animal Facility with free access to food and water prior to assessment of myocardial morphology and function. Rectal temperature was monitored weekly to assure adequate body core temperature. Systolic and diastolic blood pressures were examined at room or cold (4°) temperature based on the mouse group assignment using a KODA semi-automated, amplified tail cuff device (Kent Scientific Corporation, Torrington, CT). Blood was collected from tail veins into heparinized tubes immediately prior to animal sacrifice. Blood samples were centrifuged at 500 rpm using a microcentrifuge to collect plasma. Plasma levels of NO, ET-1, norepinephrine and TGF-β were measured using NO analyzing system or commercial ELISA kits.

Catalase Activity

Tissues were homogenized in 1% Triton X-100 containing assay buffer using a variable-speed tissue tearer (Biospec Products, Racine, WI, USA) at 20,000 rpm for 30 sec. The homogenates were centrifuged at 6000 g at 4°C for 20 min. The supernatant was diluted with 1.5 volumes of the assay buffer (50 mM KH_2PO_4/50 mM Na_2HPO_4, pH 7.0). The enzyme activity was determined by adding 1 ml 30 mM H_2O_2 to 2 ml of sample and the change in absorbance at 240 nm was monitored at 25°C for 1 min. Specific activity is expressed as μmol H_2O_2/min/mg protein [32]

Determination of reduced and oxidized glutathione (GSH and glutathione disulfide [GSSG])

The heart glutathione contents were measured as described [33]. Tissue samples (~50 mg) were sonicated in picric acid and centrifuged at 13,500 × g for 20 min. The supernatant was then divided into two aliquots. One was directly used for total GSH assay and the other for GSSG. 100 μl of supernatant fractions with 2 μl vinyl pyridine were incubated at room temperature for 1 hr to scavenge GSH for the GSSG determination. The GSSG was then subtracted from the total glutathione to evaluate the GSH levels. GSH was determined by the DTNB-glutathione reductase recycling mechanism [33].

Echocardiographic assessment

Cardiac geometry and function were evaluated in anesthetized (Avertin 2.5%, 7 μl/g body weight, i.p.) mice using the 2-D guided M-mode echocardiography (Sonos 5500) equipped with a 15–6 MHz linear transducer at room or cold (4°) temperature based on the mouse group assignment. Left ventricular (LV) anterior and posterior wall dimensions during diastole and systole were recorded from three consecutive cycles in M-mode using the methods adopted by the American Society of Echocardiography. Fractional shortening was calculated from LV end-diastolic (EDD) and end-systolic (ESD) diameters using the equation (EDD-ESD)/EDD. Heart rates were averaged over 30 consecutive cardiac cycles [34].

Isolation of murine cardiomyocytes and in vitro TGF-β treatment

After ketamine/xylazine sedation (ketamine 80 mg/kg and xylazine 12 mg/kg, i.p.), hearts were removed and perfused with Krebs-Henseleit bicarbonate (KHB) buffer at room temperature containing (in mM): 118 NaCl, 4.7 KCl, 1.2 $MgSO_4$, 1.2 KH_2PO_4, 25 $NaHCO_3$, 10 HEPES and 11.1 glucose. Hearts were digested with collagenase D for 20 min. Left ventricles were removed and minced before being filtered. Myocyte yield was ~ 75% which was not affected by low ambient temperature exposure or metallothionein transgene. Only rod-shaped myocytes with clear edges were selected for mechanical and intracellular Ca^{2+} study [34]. To evaluate the direct impact of the cell proliferation cytokine TGF-β on cardiomyocyte mechanics, a cohort of cardiomyocytes isolated from normal temperature-

maintained FVB mice was exposed to TGF-β (2 ng/ml) for 6 hrs [35] prior to the assessment of cardiomyocyte contractile function. Longer incubation duration was not chosen due to the rapid deterioration of cardiomyocyte mechanics after 8 hrs of cell isolation.

Cell shortening/relengthening

Mechanical properties of cardiomyocytes were assessed using an IonOptix™ soft-edge system (IonOptix, Milton, MA, USA). Myocytes were placed in a chamber mounted on the stage of an Olympus IX-70 microscope and superfused (~2 ml/min at 25°C) with a KHB buffer containing 1 mM $CaCl_2$. Myocytes were field stimulated at 0.5 Hz. Cell shortening and relengthening were assessed including peak shortening (PS), time-to-PS (TPS), time-to-90% relengthening (TR_{90}) and maximal velocities of shortening/relengthening (± dL/dt) [36].

Intracellular Ca^{2+} transients

A cohort of myocytes was loaded with fura-2/AM (0.5 μM) for 10 min and fluorescence intensity were recorded with a dual-excitation fluorescence photomultiplier system (Ionoptix). Myocytes were placed onto an Olympus IX-70 inverted microscope and imaged through a Fluor × 40 oil objective. Cells were exposed to light emitted by a 75W lamp and passed through either a 360 or a 380 nm filter, while being stimulated to contract at 0.5 Hz. Fluorescence emissions were detected between 480–520 nm and qualitative change in fura-2 fluorescence intensity (FFI) was inferred from the FFI ratio at the two wavelengths (360/380). Fluorescence decay time (both single and bi-exponential curve fit) was calculated as an indicator of intracellular Ca^{2+} clearing [36].

Histological examination

Following anesthesia, hearts were excised and immediately placed in 10% neutral-buffered formalin at room temperature for 24 hrs after a brief rinse with PBS. The specimen were embedded in paraffin, cut in 5 μm sections and stained with Masson's trichrome to detect fibrosis in myocardial sections. The percentage of fibrosis was calculated using the histogram function of the photoshop software. Briefly, 7 random fields (6 mm^2) at 200× magnification from each section were assessed for fibrosis. The fraction of the light blue stained area normalized to the total area was used as an indicator of myocardial fibrosis while omitting fibrosis of the perivascular, epicardial and endocardial areas from the calculation [37].

Myocardial collagen crosslinking

Collagen solubility was analyzed using our previously described method [38]. Briefly, left ventricular samples were minced to an approximate of 3–4 mm and mixed with 1 ml of 250 μg/ml pepsin in 0.5 M acetic acid at 37°C. After 2 hrs of pepsin digestion, a condition reported to cause solubilization of unmodified heart collagen, 200 μl of supernatant was removed and hydroxyproline concentration was measured using the hydroxyproline assay buffer. Optical absorbance was obtained with a spectrophotometer at 557 nm. Total recoverable myocardial collagen content was determined by hydroxyproline concentration following acid hydrolysis (6 M HCl at 110°C). Collagen solubility was expressed as hydroxyproline levels normalized to total recoverable collagen after acid hydrolysis.

Intracellular ROS measurement

Cardiomyocytes were loaded with 5-(6)-chloromethyl-2',7'-dichlorodihydrofluorescein diacetate (CM-H_2DCFDA, 1 μM) (Molecular Probes, Eugene, OR, USA) for 30 min at 37°C for detection of intracellular ROS. Cells were sampled randomly using an Olympus BX-51 microscope equipped with Olympus MagnaFire™ SP digital camera and ImagePro

image analysis software (Media Cybernetics, Silver Spring, MD, USA). Fluorescence was calibrated with InSpeck microspheres (Molecular Probes). An average of 100 cells was evaluated using the grid crossing method in 15 visual fields per isolation.

TUNEL assay

TUNEL staining of myonuclei positive for DNA strand breaks were determined using a fluorescence detection kit (Roche, Indianapolis, IN, USA). Paraffin-embedded sections (5 μm) were deparaffinized and rehydrated before incubation with Proteinase K solution at room temperature for 30 min. TUNEL reaction mixture containing terminal deoxynucleotidyl transferase (TdT), fluorescein-dUTP was added to the sections in 50-μl drops and incubated for 60 min at 37°C in a humidified chamber in the dark. Following embedding, sections were visualized with an Olympus BX-51 microscope equipped with an Olympus MaguaFire SP digital camera. DNase I and label solution were used as positive and negative controls. To determine the percentage of apoptotic cells, micrographs of TUNEL-positive and DAPI-stained nuclei were captured using an Olympus fluorescence microscope and counted using the ImageJ software (ImageJ version 1.43r; NIH) from 15 random fields at 400× magnification [39].

Western blot analysis

The protein was prepared as described [33]. Samples containing equal amount of proteins were separated on 10% SDS-polyacrylamide gels in a minigel apparatus (Mini-PROTEAN II, Bio-Rad, Hercules, CA, USA) and transferred to nitrocellulose membranes. The membranes were blocked with 5% milk in TBS-T, and were incubated overnight at 4°C with anti-HIF-1α, anti-SOD1, anti-eNOS, anti-AT_1 receptor, anti-Bax, anti-Bcl-xl, anti-Bip, anti-Calregulin, anti-IRE1α, anti-phospho-IRE1α (Ser724), anti-eIF2α, anti-phospho-eIF2α (Ser51), anti-CHOP, anti-caspase-12, anti-MMP-2, anti-MMP-9 anti-TGF-β, anti-Smad-2/3 and anti-metallothionein antibodies. After immunoblotting, the film was scanned and the intensity of immunoblot bands was detected with a Bio-Rad Calibrated Densitometer. GAPDH was used as the loading control. To avoid the potential impact of abrupt hemodynamic change, tissue collection was performed in cold room for the cold temperature groups.

Cardiac fibroblast isolation, metallothionein induction and proliferation assay

To examine the effect of metallothionein on fibrosis, cardiac fibroblasts were exposed to the cell proliferation inducer TGF-β *in vitro* prior to determination of cell proliferation. In brief, hearts were removed from normal FVB mice. After being washed with PBS, heart tissues were minced and digested in 0.25% collagenase solution at 37°C for 1 hr. After digestion, cells were pelleted by centrifugation at 1,500 rpm for 10 min and suspended in DMEM supplemented with 1% penicillin/streptomycin and 10% fetal bovine serum. The suspension was then transferred to a culture dish. After 1 hr of incubation at 37°C, cells that were weakly attached or unattached were removed, and the attached cells were cultured in the dish with DMEM. The purity of these cultured cardiac fibroblasts was > 90% on the basis of positive staining for vimentin and negative staining for smooth muscle cell α-actin and von Willebrand factor. Cardiac fibroblasts cultured to the fifth passage were used in our study [40]. Given the difficulty of metallothionein to penetrate through the cell membrane, Zinc was employed to induce metallothionein in primary fibroblasts by exposing cells to 50 μM $ZnCl_2$ for 24 hrs [16]. Expression of metallothionein was confirmed using western blot analysis. Cells with or without metallothionein induction were then incubated with pro-oxidant H_2O_2 (50 μM) [41] or TGF-β (2 ng/ml) [35] for 24 hrs. A cohort of fibroblasts were pretreated with the TGF-β-Smad-2/3 signaling inhibitor SB431542 (10 μM) [42] or the TGF-β neutralizing antibody (0.1 μg/ml) [43] for 2 hrs prior to H_2O_2 challenge (50 μM for 24hrs). Equal volume of solute for these reagents was used as vehicle (which displays no

effect on cell proliferation). Cell growth of fibroblasts was assessed by 3-(4,5-dimethylthiazol-2-yl) -2,5-diphenyltetrazolium bromide (MTT) assay. Cell number was determined in triplicate using a hemocytometer. Results were shown as MTT conversion normalized to cell number in vehicle control group (as 100%).

To further delineate the causality in the cellular signaling mechanism involved in metallothionein-offered action on cold exposure-induced myocardial fibrosis, if any, the effects of pro-oxidant H_2O_2 and TGF-β on cardiac fibroblast proliferation were examined *in vitro* in fibroblasts isolated from FVB mice in the presence or absence of metallothionein induced by zinc chloride [16] or inhibitor (or neutralizing antibody) of TGF-β or Smad-2/3. Our transgenic model of metallothionein is cardiomyocyte-specific without overexpression in fibroblasts.

Data analysis

Data were mean ± SEM. Statistical significance ($p < 0.05$) was estimated by a two-way analysis of variance (ANOVA) followed by a Bonferroni multi-comparison analysis when necessary.

RESULTS

Biometric profile and antioxidant capacity in FVB and metallothionein transgenic mice

Chronic cold exposure significantly enhanced or decreased, respectively, plasma levels of epinephrine and NO, the effects of which were unaffected by metallothionein. Neither cold exposure nor metallothionein, or both, affected plasma ET-1 levels (Fig. 1A–C). Assessment of myocardial antioxidant capacity revealed that cold exposure significantly reduced the levels of SOD1, catalase activity and glutathione (low GSH-to-GSSG ratio), the effects of which were reversed by metallothionein (Fig. 1D–F). Given that cold exposure may affect HIF-1α, eNOS and angiotensin II cascade [21, 22], levels of HIF-1α, eNOS and angiotensin II receptor (AT_1) were evaluated. Cold exposure significantly increased HIF-1α expression and decreased eNOS level in the heart, the effects of which were mitigated by metallothionein. Neither cold exposure nor metallothionein, or both, produced any notable effect on AT_1 receptor expression (Fig. 1G–I). Metallothionein itself did not elicit any effect on plasma levels of norepinephrine, ET-1 and NO, myocardial levels of SOD1, catalase, glutathione, HIF-1α, eNOS and AT_1 receptor. In addition, cold exposure did not affect diastolic blood pressure (FVB-normal temperature: 81.6 ± 5.8 mmHg; FVB-low temperature: 89.5 ± 6.5 mmHg; MT-normal temperature: 82.4 ± 4.7 mmHg; MT-low temperature: 85.9 ± 8.1 mmHg; n = 9 – 13 mice per group, $p > 0.05$). However, chronic cold exposure significantly elevated the systolic blood pressure, the effect of which was unaffected by metallothionein (FVB-normal temperature: 115.3 ± 7.9 mmHg; FVB-low temperature: 160.7 ± 10.4 mmHg; MT-normal temperature: 116.0 ± 6.9 mmHg; MT-low temperature: 154.8 ± 15.9 mmHg; n = 9 – 13 mice per group, two–way ANOVA: temperature: $p < 0.05$; mouse gene: $p > 0.05$; temperature × mouse gene: $p > 0.05$). Cold exposure significantly elevated the plasma TGF-β, the effect of which was unaffected by metallothionein (FVB-normal temperature: 1.82 ± 0.12 ng/ml; FVB-low temperature: 3.03 ± 0.21 ng/ml; MT-normal temperature: 1.75 ± 0.14 ng/ml; MT-low temperature: 3.14 ± 0.22 ng/ml; n = 8 – 10 mice per group, two–way ANOVA: temperature: $p < 0.05$; mouse gene: $p > 0.05$; temperature × mouse gene: $p > 0.05$).

Echocardiographic properties of FVB and metallothionein transgenic mice

Our data shown in Fig. 2 revealed that neither cold exposure nor metallothionein affected body weight, heart weight, heart rate, LV mass (absolute value or when normalized to body weight), LV wall thickness and LV end diastolic diameter (LVEDD). Extremely cold

exposure significantly increased LV end systolic diameter (LVESD) and reduced fractional shortening in FVB mice, the effect of which was abrogated by metallothionein overexpression. Metallothionein itself did not elicit any notable effect on LVESD and fractional shortening.

Cardiomyocyte contractile and intracellular Ca^{2+} property in FVB and metallothionein mice

Cold exposure but not metallothionein significantly enhanced resting cell length. There was a further increase in resting cell length in the cold-exposed metallothionein mice compared with the cold-exposed FVB mice. Cold exposure significantly dampened peak shortening (PS) and maximal velocity of shortening/relengthening (± dL/dt) as well as prolonged time-to-90% relengthening (TR_{90}) without affecting time-to peak shortening (TPS) in FVB mice. Unlike its echocardiographic effects, metallothionein transgene failed to alter cold exposure-induced mechanical abnormalities nor did it elicit any notable mechanical effects by itself (Fig. 3). Furthermore, cardiomyocytes from mice exposed to cold temperature displayed a significantly elevated baseline intracellular Ca^{2+}, depressed intracellular Ca^{2+} rise in response to electrical stimulus (ΔFFI) and reduced intracellular Ca^{2+} decay rate (both single and bi-exponential). Metallothionein overexpression failed to negate the cold exposure-induced intracellular Ca^{2+} mishandling and did not affect the intracellular Ca^{2+} properties by itself (Fig. 4).

Effect of metallothionein on cold exposure-induced myocardial histological change

To assess the effect of metallothionein overexpression on myocardial histology following cold exposure, myocardial fibrosis was examined. Findings from the Masson Trichrome staining revealed that cold exposure elicited overt myocardial fibrosis, the effect of which was partially attenuated by metallothionein. This was supported by a greater myocardial collagen crosslinking (shown as lower collagen solubility) following cold exposure, the effect of which was obliterated by metallothionein. The heavy metal scavenger itself did not affect myocardial fibrosis or collagen crosslinking (Fig. 5).

Effects of metallothionein on cold exposure-induced ROS production and apoptosis

To examine the potential mechanism of action behind metallothionein-elicited protection against cold exposure-induced myocardial contractile dysfunction, generation of ROS and apoptosis was examined in cardiomyocytes or myocardium from FVB and metallothionein mice with cold exposure. Results shown in Fig. 6A–D indicate that generation of ROS and expression of the pro-apoptotic protein Bax were significantly elevated in cold exposed FVB group. Consistent with its echocardiographic responses, metallothionein nullified cold exposure-induced ROS generation but failed to affect the upregulated Bax expression. Metallothionein itself exerted minimal effects on ROS generation and Bax expression in the absence of cold exposure. Neither cold exposure nor metallothionein overexpression affected the expression of the anti-apoptotic protein Bcl-xl. Interestingly, TUNEL staining revealed that metallothionein transgene partially attenuated cold exposure-induced increase in the TUNEL positive cells (depicting apoptosis) without eliciting any effect by itself (Fig. 6E–F).

Western blot analysis of ER stress markers in FVB and metallothionein mice

To elucidate the possible mechanism(s) involved in the metallothionein-elicited protection against cold exposure-induced cardiac contractile dysfunction, we examined the expression of the ER stress protein markers Bip, calregulin, CHOP, pan and phosphorylated forms of IRE1α and eIF2α, as well as the ER-specific member of the caspase family - caspase-12 [44]. As shown in Fig. 7, chronic cold exposure led to downregulated protein expression of Bip, Calregulin and eIF2α phosphorylation without affecting that of CHOP, IRE1α (pan

and phosphorylated) and pan eIF2α. Although metallothionein itself failed to affect any of the ER stress markers tested, it significantly attenuated cold exposure-induced decrease in calregulin but not Bip and phosphorylated eIF2α. In addition, metallothionein significantly downregulated CHOP without affecting the levels of pan and phosphorylated IRE1α under cold exposure. Expression of caspase-12 was significantly upregulated following chronic cold exposure, the effect of which was significantly attenuated by metallothionein overexpression. Last but not least, metallothionein itself did not affect the protein expression of caspase-12.

Western blot analysis of MMP-2/MMP-9, TGF-β and Smad-2/3 in FVB and metallothionein mice

To explore the mechanism(s) of action behind metallothionein-induced inhibition of cardiac fibrosis, expression of the profibrotic matrix metalloproteinases MMP-2 and MMP-9 was examined in FVB and metallothionein mouse hearts following cold exposure. Our results depicted that cold exposure significantly upregulated the expression of both MMP-2 and MMP-9, consistent with the increased fibrosis. While metallothionein itself did not affect the expression of MMP-2 and -9, it ablated cold exposure-induced changes in MMP-2 and MMP-9. Given that the cell proliferative cytokine TGF-β was shown to be associated with cold stress [45] and is well known for its role in promoting pro-collagen genes and synthesis of extracellular matrix *en route* to cardiac fibrosis [25–27], levels of TGF-β and Smad-2/3, the initiation factor of TGF-β-mediated fibrosis, were examined in FVB and metallothionein mouse hearts following cold exposure. Consistent with the findings of MMP-2/9, levels of TGF-β and Smad-2/3 were significantly upregulated following cold exposure, the effects of which were ablated by metallothionein overexpression in the heart. Last but not least, the antioxidant itself did not affect the levels of TGF-β and Smad-2/3 by itself (Fig. 8A–D).

Effect of induced metallothionein on TGF-β and H_2O_2-induced fibroblast proliferation

Cardiac fibrosis involves an increase in collagen synthesis, proliferation of fibroblasts or a decrease in collagen degradation [25, 27]. To investigate the mechanism behind the antifibrotic effect of metallothionein, we examined the effect of metallothionein induction using Zinc [16] on fibroblast proliferation. *In vitro* incubation of Zinc (50 μM) for 24 hrs significantly increased the protein abundance of metallothionein in fibroblasts confirmed using Western blot analysis (Optical density normalized to GAPDH: Control: 1.08 ± 0.09; Zinc: 4.27 ± 0.34, n = 4 isolation, $p < 0.05$ *vs.* control group). Given the elevated cardiac expression of the cell proliferative cytokine TGF-β in our study as shown previously in cold stress [45] and its known role in promoting pro-collagen genes and synthesis of extracellular matrix *en route* to cardiac fibrosis [25–27], TGF-β (2 ng/ml)-induced cell growth was performed using cardiac fibroblasts isolated from normal temperature-maintained FVB mice with or without metallothionein induction. The pro-oxidant H_2O_2 (50 μM) was used as a positive control for ROS accumulation and oxidative stress. Our data revealed that metallothionein induction using Zinc treatment nullified H_2O_2- but not TGF-β-elicited cell proliferation (Fig. 8E). To further elucidate the potential signaling mechanism involved in oxidative- and/or TGF-β-induced cell proliferation, cardiac fibroblasts were exposed to H_2O_2 (50 μM) for 24 hrs in the absence or presence of the inhibitor or neutralizing antibody of the TGF-β-Smad-2/3signaling cascade. Our data shown in Fig. 8F revealed that both neutralizing antibody for TGF-β and the TGF-β-Smad-2/3 signaling inhibitor SB431542 abolished H_2O_2-elicited proliferative responses. Lastly, neither metallothionein induction nor neutralizing antibody of TGF-β-or SB431542 exerted any notable proliferative effect in cardiac fibroblasts.

Influence of TGF-β on cardiomyocyte contractile function in FVB and metallothionein mice

To evaluate the impact of the elevated TGF-β following cold exposure on cardiomyocyte contractile response, cardiomyocyte shortening/relengthening was evaluated in cardiomyocytes incubated with TGF-β (2 ng/ml) for 6 hrs. Our data shown in Fig. 9 depicted that comparable resting cell length in the FVB and metallothionein murine cardiomyocytes treated with or without TGF-β. TGF-β overtly dampened PS and ± dL/dt as well as prolonged TR_{90} without affecting TPS in a comparable manner in cardiomyocytes from both FVB and metallothionein transgenic mice, suggesting little effect of the antioxidant on TGF-β-induced cardiomyocyte dysfunction.

DISCUSSION

The salient findings from our study revealed that metallothionein significantly improved cold exposure-induced myocardial contractile dysfunction. Our data revealed that metallothionein significantly ameliorated ROS generation and cardiac fibrosis as well as partially alleviated apoptosis following cold exposure despite persistent cardiomyocyte contractile and intracellular Ca^{2+} derangement. These findings indicate a role of ROS and fibrosis in cold exposure-induced cardiac abnormalities. In addition, metallothionein ablated cold exposure-induced increases in the levels of collagen crosslinking, extracellular matrix metalloproteinase MMP-2/-9, cell proliferative cytokine TGF-β (heart but not plasma) and the initiation factor of TGF-β-induced fibrotic response namely Smad-2/3. Interestingly, *in vitro* metallothionein induction using Zinc effectively abrogated oxidative stress but not TGF-β-induced cell proliferation in cardiac fibroblasts. These data favor the notion that suppression of fibrosis resulted from oxidative stress and cardiac TGF-β accumulation may contributes to metallothionein-elicited protection against cold exposure-induced myocardial anomalies. Our findings indicate the therapeutic potential of antioxidants in the treatment against cold exposure-induced cardiovascular complications.

Cold stress has been shown to affect blood pressure and increases blood viscosity, which may in turn lead to the onset of stroke and acute myocardial infarction [46]. Individuals residing in cold climates usually display a higher prevalence of cardiovascular diseases [47–50]. Our data revealed that cold exposure for 3 months increased plasma levels of norepinephrine, ET-1, and TGF-β levels, while decreasing plasma NO levels (as well as cardiac eNOS abundance) with change in cardiac AT_1 level, consistent with the previous reports [22, 29, 45, 51]. In addition, cold exposure enhanced systolic blood pressure and triggered cardiac contractile dysfunction. Long-term (1 year) cold exposure has been confirmed to promote ROS generation accompanied with a compensatory increase in antioxidant enzymes [11]. This is consistent with our observation of enhanced ROS production and overt apoptosis in myocardium following cold challenge. Interestingly, our data revealed a reduced antioxidant defense capacity (SOD1, catalase and glutathione) following the 3-month cold exposure, suggesting difference in antioxidant defense with time of cold exposure. Although cold exposure was indicated to be associated with ER stress [20], data from our study suggested reduced (Bip, Calregulin and eIF2α phosphorylation) or unchanged (CHP and IRE1α phosphorylation) ER stress protein markers following cold stress. Although the precise mechanism behind cold stress-induced reduction in ER stress markers is still unclear, the reduced ER stress may represent a possible compensatory mechanism to counter cold stress-induced injury. The fact that cold exposure overtly upregulated the ER-specific apoptotic caspase-12 in the absence of overt ER stress may depict (1) an ER stress-independent mechanism in caspase-12 elevation; or (2) a compensatory decrease in ER stress proteins as a result of ER stress following sustained cold exposure. Our data observed overt apoptosis (TUNEL and Bax expression) without any change in the B-cell lymphoma-extra large (Bcl-xl) following cold exposure, thus not favoring a major role of Bcl-xl in our present experimental setting. Bcl-xl, a transmembrane

molecule in mitochondria, is an anti-apoptotic protein in the Bcl-2 family (along with other Bcl-2 proteins including Bcl-2, Bcl-w, Bcl-xs, and Mcl-1) [52, 53]. Our data suggest a pivotal role of ROS production in cold exposure-induced apoptosis and fibrosis (Masson Trichrome staining, collagen crosslinking, MMPs, TGF-β and Smad-2/3). Oxidative stress and ROS accumulation promote cardiac fibrosis via a TGF-β-mediated mechanism [25, 27, 28, 54]. Although ROS has also been reported to mediate TGF-β-induced cell proliferative response [55], it is believed that TGF-β may sense certain types of oxidative stress to trigger pro-inflammatory and proliferative responses in extracellular cellular matrix in response to ROS production and oxidative stress [54]. This is supported by our finding that metallothionein failed to rescue against TGF-β-induced fibroblast proliferation and cardiomyocyte dysfunction, and that TGF-β inhibition using neutralizing antibody ablated H_2O_2-induced fibroblast proliferation. These data depict a possible downstream role of TGF-β in oxidative stress-induced fibroblast proliferation. However, possible involvement of ROS downstream of TGF-β cannot be excluded as certain ROS species may not be eradicated by metallothionein.

Finding from our study has indicated that metallothionein reversed cold exposure-induced myocardial contractile function in the absence of improvement in cardiomyocyte contractile function and intracellular Ca^{2+} properties. Although the discrepancy between the whole heart and individual cardiomyocyte findings is not entirely clear, the fact that metallothionein lessened cold exposure-induced cardiac fibrosis, collagen crosslinking, increase in tissue TGF-β/Smad-2/3 and upregulation of MMP-2/-9 but not plasma TGF-β levels and TGF-β-induced cardiomyocyte dysfunction. These data prompt a role of TGF-β/Smad-mediated fibrosis in metallothionein-elicited protection against cold exposure-induced myocardial anomalies. This is in concert with the findings that TGF-β-Smad-2/3 signaling inhibition mitigated H_2O_2-induced cardiac fibroblast proliferation, suggesting that metallothionein may exert its beneficial role likely through inhibition of ROS and subsequently local TGF-β accumulation. Cold exposure is associated with rises in TGF-β levels and oxidative stress [42, 45], as shown in our study. Not surprisingly, cardiac-specific overexpression of metallothionein cannot reconcile the elevated plasma levels of TGF-β along with the changes in norepinephrine, ET-1, NO and AT_1 receptor, not favoring a systemic effect of metallothionein against cold exposure. Cardiac metallothionein overexpression protects against cold-induced local eNOS expression with little effect on circulating NO levels. Studies using genetic models confirmed the involvement of TGF-β in cardiac hypertrophy and interstitial fibrosis [56]. Cardiac fibroblasts respond to ROS to promote proinflammatory cytokines including TNF-α, IL-1, IL-6 and TGF-β, the levels of which are increased in remodeling hearts, to initiate tissue repair [27, 54]. Activation of the Smad signaling has been shown to play an important role in TGF-β-induced apoptosis and fibrosis [29]. Our data revealed that SB431542 ablated H_2O_2-induced fibroblast proliferation, suggesting a role of Smad-2/3 in oxidative stress-induced myocardial fibrosis. Given the nature of cardiomyocyte-specific overexpression for metallothionein [18, 30], our data favor the notion that metallothionein inhibits cardiac fibrosis through a ROS-mediated suppression in the levels of TGF-β, Smad-2/3 and MMP-2/-9 in the heart.

Cold temperature affects hemodynamic properties of the cardiovascular system to trigger cardiovascular complications (stroke, myocardial infarction, and heart failure) [31]. Data from our study revealed elevated systolic blood pressure associated with unchanged diastolic blood pressure following cold exposure. Echocardiographic findings revealed enlarged LV ESD but not LV EDD following cold exposure. Enlarged LV ESD may be related to the increased afterload (systolic blood pressure). Although presence of cardiac fibrosis in cold-exposed mice is expected to enhance ventricular stiffness and thus enlarged LV EDD, the unchanged LV EDD associated with cardiac fibrosis may be due to compensatory mechanisms and the relatively short duration of cold exposure. In our hand, metallothionein

restored LV ESD and myocardial function despite persistent systolic hypertension, not favoring systolic blood pressure as the sole determining factor in metallothionein-induced protection against cold exposure-induced cardiac remodeling and contractile anomalies. Although it is beyond the scope of our current study, upregulation of HIF-1α in response to cold exposure and oxidative stress [21], as seen in our study, was reported to promote collagen deposition [57]. Therefore, it is possible that the heavy metal scavenger may counteract cardiac fibrosis in part through regulation of HIF-1α-mediated collagen deposition.

Experimental limitation: One of the main experimental limitations for our present study is the inability to obtain pure isolated cardiomyocytes or fibroblasts used for Western blot analysis. The immunoblotting result of apoptosis and ER stress as well as that for TUNEL assay are derived from whole heart homogenates comprised of both cardiomyocytes and fibroblasts (mainly cardiomyocytes). Therefore, apoptosis measured may reflect a combination of both cell types (e.g., apoptotic cardiomyocytes in conjunction with proliferative cardiac fibroblasts). In addition, use of the 15-MHz probe for echocardiographic evaluation does not provide an optimal resolution. Caution should be taken with LV mass derived from the echocardiographic recording.

In summary, our study provides evidence that metallothionein overexpression rescues cold exposure-induced myocardial remodeling and contractile dysfunction despite persistent cardiomyocyte contractile and intracellular Ca^{2+} derangements. Our data indicated that ROS generation, TGF-β, Smad-2/3 and MMP-2/-9, and resulted cardiac fibrosis may play an essential role in cold exposure and metallothionein overexpression-elicited changes in cardiac contractile function. Given the role of antioxidants in the protection against cardiac anomalies [12, 13, 18, 58], our data suggest the therapeutic potential of antioxidants in the management of cold stress-associated myopathic complications.

Acknowledgments

The authors wish to acknowledge Ms. Sara A. Babcock for technical assistance. This work was supported by NIH P20 RR016474 (JR).

Reference List

[1]. Cold exposure and winter mortality from ischaemic heart disease, cerebrovascular disease, respiratory disease, and all causes in warm and cold regions of Europe. The Eurowinter Group. Lancet. 1997; 349:1341–1346. [PubMed: 9149695]

[2]. Abrignani MG, Corrao S, Biondo GB, Renda N, Braschi A, Novo G, Di Girolamo A, Braschi GB, Novo S. Influence of climatic variables on acute myocardial infarction hospital admissions. International journal of cardiology. 2009; 137:123–129. [PubMed: 18694607]

[3]. Barnett AG, Dobson AJ, McElduff P, Salomaa V, Kuulasmaa K, Sans S. Cold periods and coronary events: an analysis of populations worldwide. J Epidemiol Community Health. 2005; 59:551–557. [PubMed: 15965137]

[4]. Huynen MM, Martens P, Schram D, Weijenberg MP, Kunst AE. The impact of heat waves and cold spells on mortality rates in the Dutch population. Environmental health perspectives. 2001; 109:463–470. [PubMed: 11401757]

[5]. Kysely J, Pokorna L, Kyncl J, Kriz B. Excess cardiovascular mortality associated with cold spells in the Czech Republic. BMC public health. 2009; 9:19. [PubMed: 19144206]

[6]. Cheng X, Su H. Effects of climatic temperature stress on cardiovascular diseases. European Journal of Internal Medicine. 21:164–167. [PubMed: 20493415]

[7]. Epstein SE, Stampfer M, Beiser GD, Goldstein RE, Braunwald E. Effects of a reduction in environmental temperature on the circulatory response to exercise in man. Implications concerning angina pectoris. N Engl J Med. 1969; 280:7–11. [PubMed: 5761728]

[8]. Juneau M, Johnstone M, Dempsey E, Waters DD. Exercise-induced myocardial ischemia in a cold environment. Effect of antianginal medications. Circulation. 1989; 79:1015–1020. [PubMed: 2713970]

[9]. Shea MJ, Deanfield JE, deLandsheere CM, Wilson RA, Kensett M, Selwyn AP. Asymptomatic myocardial ischemia following cold provocation. Am Heart J. 1987; 114:469–476. [PubMed: 3498354]

[10]. Cheng X, Su H. Effects of climatic temperature stress on cardiovascular diseases. Eur J Intern Med. 2010; 21:164–167. [PubMed: 20493415]

[11]. Hong JH, Kim KJ, Suzuki K, Lee IS. Effect of cold acclimation on antioxidant status in cold acclimated skaters. J Physiol Anthropol. 2008; 27:255–262. [PubMed: 18838841]

[12]. Cai L, Wang Y, Zhou G, Chen T, Song Y, Li X, Kang YJ. Attenuation by metallothionein of early cardiac cell death via suppression of mitochondrial oxidative stress results in a prevention of diabetic cardiomyopathy. J Am Coll Cardiol. 2006; 48:1688–1697. [PubMed: 17045908]

[13]. Dong F, Li Q, Sreejayan N, Nunn JM, Ren J. Metallothionein prevents high-fat diet induced cardiac contractile dysfunction: role of peroxisome proliferator activated receptor gamma coactivator 1alpha and mitochondrial biogenesis. Diabetes. 2007; 56:2201–2212. [PubMed: 17575086]

[14]. Fang CX, Dong F, Ren BH, Epstein PN, Ren J. Metallothionein alleviates cardiac contractile dysfunction induced by insulin resistance: role of Akt phosphorylation, PTB1B, PPARgamma and c-Jun. Diabetologia. 2005; 48:2412–2421. [PubMed: 16172869]

[15]. Fang CX, Doser TA, Yang X, Sreejayan N, Ren J. Metallothionein antagonizes aging-induced cardiac contractile dysfunction: role of PTP1B, insulin receptor tyrosine phosphorylation and Akt. Aging Cell. 2006; 5:177–185. [PubMed: 16626396]

[16]. Wang J, Song Y, Elsherif L, Song Z, Zhou G, Prabhu SD, Saari JT, Cai L. Cardiac metallothionein induction plays the major role in the prevention of diabetic cardiomyopathy by zinc supplementation. Circulation. 2006; 113:544–554. [PubMed: 16432057]

[17]. Wang Y, Feng W, Xue W, Tan Y, Hein DW, Li XK, Cai L. Inactivation of GSK-3beta by metallothionein prevents diabetes-related changes in cardiac energy metabolism, inflammation, nitrosative damage, and remodeling. Diabetes. 2009; 58:1391–1402. [PubMed: 19324938]

[18]. Yang X, Doser TA, Fang CX, Nunn JM, Janardhanan R, Zhu M, Sreejayan N, Quinn MT, Ren J. Metallothionein prolongs survival and antagonizes senescence-associated cardiomyocyte diastolic dysfunction: role of oxidative stress. FASEB J. 2006; 20:1024–1026. [PubMed: 16585059]

[19]. Hu N, Guo R, Han X, Zhu B, Ren J. Cardiac-specific overexpression of metallothionein rescues nicotine-induced cardiac contractile dysfunction and interstitial fibrosis. Toxicol Lett. 2011; 202:8–14. [PubMed: 21238558]

[20]. Williams B, Kabbage M, Britt R, Dickman MB. AtBAG7, an Arabidopsis Bcl-2-associated athanogene, resides in the endoplasmic reticulum and is involved in the unfolded protein response. Proc Natl Acad Sci U S A. 2010; 107:6088–6093. [PubMed: 20231441]

[21]. Heise K, Estevez MS, Puntarulo S, Galleano M, Nikinmaa M, Portner HO, Abele D. Effects of seasonal and latitudinal cold on oxidative stress parameters and activation of hypoxia inducible factor (HIF-1) in zoarcid fish. Journal of comparative physiology. B, Biochemical, systemic, and environmental physiology. 2007; 177:765–777.

[22]. Sun Z. Cardiovascular responses to cold exposure. Front Biosci (Elite Ed). 2010; 2:495–503. [PubMed: 20036896]

[23]. Pei Z, Meng R, Li G, Yan G, Xu C, Zhuang Z, Ren J, Wu Z. Angiotensin-(1–7) ameliorates myocardial remodeling and interstitial fibrosis in spontaneous hypertension: role of MMPs/TIMPs. Toxicol Lett. 2010; 199:173–181. [PubMed: 20837116]

[24]. Spallarossa P, Altieri P, Garibaldi S, Ghigliotti G, Barisione C, Manca V, Fabbi P, Ballestrero A, Brunelli C, Barsotti A. Matrix metalloproteinase-2 and -9 are induced differently by doxorubicin in H9c2 cells: The role of MAP kinases and NAD(P)H oxidase. Cardiovasc Res. 2006; 69:736–745. [PubMed: 16213474]

[25]. Creemers EE, Pinto YM. Molecular mechanisms that control interstitial fibrosis in the pressure-overloaded heart. Cardiovasc Res. 2011; 89:265–272. [PubMed: 20880837]

[26]. Leask A. Potential therapeutic targets for cardiac fibrosis: TGFbeta, angiotensin, endothelin, CCN2, and PDGF, partners in fibroblast activation. Circulation research. 2010; 106:1675–1680. [PubMed: 20538689]

[27]. Porter KE, Turner NA. Cardiac fibroblasts: at the heart of myocardial remodeling. Pharmacol Ther. 2009; 123:255–278. [PubMed: 19460403]

[28]. Iglesias-De La Cruz MC, Ruiz-Torres P, Alcami J, Diez-Marques L, Ortega-Velazquez R, Chen S, Rodriguez-Puyol M, Ziyadeh FN, Rodriguez-Puyol D. Hydrogen peroxide increases extracellular matrix mRNA through TGF-beta in human mesangial cells. Kidney international. 2001; 59:87–95. [PubMed: 11135061]

[29]. Burch ML, Zheng W, Little PJ. Smad linker region phosphorylation in the regulation of extracellular matrix synthesis. Cell Mol Life Sci. 2011; 68:97–107. [PubMed: 20820849]

[30]. Ye G, Metreveli NS, Ren J, Epstein PN. Metallothionein prevents diabetes-induced deficits in cardiomyocytes by inhibiting reactive oxygen species production. Diabetes. 2003; 52:777–783. [PubMed: 12606520]

[31]. Chen GF, Sun Z. Effects of chronic cold exposure on the endothelin system. J Appl Physiol. 2006; 100:1719–1726. [PubMed: 16384835]

[32]. Ge W, Zhang Y, Han X, Ren J. Cardiac-specific overexpression of catalase attenuates paraquat-induced myocardial geometric and contractile alteration: role of ER stress. Free Radic Biol Med. 2010; 49:2068–2077. [PubMed: 20937379]

[33]. Guo R, Ma H, Gao F, Zhong L, Ren J. Metallothionein alleviates oxidative stress-induced endoplasmic reticulum stress and myocardial dysfunction. J Mol Cell Cardiol. 2009; 47:228–237. [PubMed: 19344729]

[34]. Ceylan-Isik AF, Zhao P, Zhang B, Xiao X, Su G, Ren J. Cardiac overexpression of metallothionein rescues cardiac contractile dysfunction and endoplasmic reticulum stress but not autophagy in sepsis. J Mol Cell Cardiol. 2010; 48:367–378. [PubMed: 19914257]

[35]. Hu C, Dandapat A, Sun L, Khan JA, Liu Y, Hermonat PL, Mehta JL. Regulation of TGFbeta1-mediated collagen formation by LOX-1: studies based on forced overexpression of TGFbeta1 in wild-type and lox-1 knock-out mouse cardiac fibroblasts. J Biol Chem. 2008; 283:10226–10231. [PubMed: 18182394]

[36]. Hua Y, Ma H, Samson WK, Ren J. Neuronostatin inhibits cardiac contractile function via a protein kinase A- and JNK-dependent mechanism in murine hearts. Am J Physiol Regul Integr Comp Physiol. 2009; 297:R682–689. [PubMed: 19553502]

[37]. Doser TA, Turdi S, Thomas DP, Epstein PN, Li SY, Ren J. Transgenic overexpression of aldehyde dehydrogenase-2 rescues chronic alcohol intake-induced myocardial hypertrophy and contractile dysfunction. Circulation. 2009; 119:1941–1949. [PubMed: 19332462]

[38]. Ma H, Li SY, Xu P, Babcock SA, Dolence EK, Brownlee M, Li J, Ren J. Advanced glycation endproduct (AGE) accumulation and AGE receptor (RAGE) up-regulation contribute to the onset of diabetic cardiomyopathy. Journal of cellular and molecular medicine. 2009; 13:1751–1764. [PubMed: 19602045]

[39]. Zhang B, Turdi S, Li Q, Lopez FL, Eason AR, Anversa P, Ren J. Cardiac overexpression of insulin-like growth factor 1 attenuates chronic alcohol intake-induced myocardial contractile dysfunction but not hypertrophy: Roles of Akt, mTOR, GSK3beta, and PTEN. Free Radic Biol Med. 2010; 49:1238–1253. [PubMed: 20678571]

[40]. Chen J, Mehta JL. Angiotensin II-mediated oxidative stress and procollagen-1 expression in cardiac fibroblasts: blockade by pravastatin and pioglitazone. Am J Physiol Heart Circ Physiol. 2006; 291:H1738–1745. [PubMed: 16714359]

[41]. Lim CK, Kalinowski DS, Richardson DR. Protection against hydrogen peroxide-mediated cytotoxicity in Friedreich's ataxia fibroblasts using novel iron chelators of the 2-pyridylcarboxaldehyde isonicotinoyl hydrazone class. Mol Pharmacol. 2008; 74:225–235. [PubMed: 18424550]

[42]. Nagyova E, Camaioni A, Scsukova S, Mlynarcikova A, Prochazka R, Nemcova L, Salustri A. Activation of cumulus cell SMAD2/3 and epidermal growth factor receptor pathways are involved in porcine oocyte-cumulus cell expansion and steroidogenesis. Mol Reprod Dev. 2011; 78:391–402. [PubMed: 21520325]

[43]. Satterwhite TS, Chong AK, Luo J, Pham H, Costa M, Longaker MT, Wyss-Coray T, Chang J. In vitro analysis of transforming growth factor-beta1 inhibition in novel transgenic SBE-luciferase mice. Ann Plast Surg. 2007; 59:207–213. [PubMed: 17667417]

[44]. Nakagawa T, Zhu H, Morishima N, Li E, Xu J, Yankner BA, Yuan J. Caspase-12 mediates endoplasmic-reticulum-specific apoptosis and cytotoxicity by amyloid-beta. Nature. 2000; 403:98–103. [PubMed: 10638761]

[45]. Sesti-Costa R, Baccan GC, Chedraoui-Silva S, Mantovani B. Effects of acute cold stress on phagocytosis of apoptotic cells: the role of corticosterone. Neuroimmunomodulation. 2010; 17:79–87. [PubMed: 19923852]

[46]. Aslam AF, Aslam AK, Vasavada BC, Khan IA. Hypothermia: evaluation, electrocardiographic manifestations, and management. The American journal of medicine. 2006; 119:297–301. [PubMed: 16564768]

[47]. Azzopardi D, Edwards AD. Hypothermia. Seminars in fetal & neonatal medicine. 2007; 12:303–310. [PubMed: 17392043]

[48]. Fregly MJ, Kikta DC, Threatte RM, Torres JL, Barney CC. Development of hypertension in rats during chronic exposure to cold. J Appl Physiol. 1989; 66:741–749. [PubMed: 2708203]

[49]. Kim JY, Jung KY, Hong YS, Kim JI, Jang TW, Kim JM. The relationship between cold exposure and hypertension. J Occup Health. 2003; 45:300–306. [PubMed: 14646271]

[50]. Lauri T, Leskinen M, Timisjarvi J, Hirvonen L. Cardiac function in hypothermia. Arctic medical research. 1991; 50(Suppl 6):63–66. [PubMed: 1811582]

[51]. Sun Z, Bello-Roufai M, Wang X. RNAi inhibition of mineralocorticoid receptors prevents the development of cold-induced hypertension. Am J Physiol Heart Circ Physiol. 2008; 294:H1880–1887. [PubMed: 18296563]

[52]. Bonavita F, Stefanelli C, Giordano E, Columbaro M, Facchini A, Bonafe F, Caldarera CM, Guarnieri C. H9c2 cardiac myoblasts undergo apoptosis in a model of ischemia consisting of serum deprivation and hypoxia: inhibition by PMA. FEBS Lett. 2003; 536:85–91. [PubMed: 12586343]

[53]. Lai KB, Sanderson JE, Yu CM. High dose norepinephrine-induced apoptosis in cultured rat cardiac fibroblast. International journal of cardiology. 2009; 136:33–39. [PubMed: 18675472]

[54]. Annes JP, Munger JS, Rifkin DB. Making sense of latent TGFbeta activation. J Cell Sci. 2003; 116:217–224. [PubMed: 12482908]

[55]. Cui Y, Robertson J, Maharaj S, Waldhauser L, Niu J, Wang J, Farkas L, Kolb M, Gauldie J. Oxidative stress contributes to the induction and persistence of TGF-beta1 induced pulmonary fibrosis. Int J Biochem Cell Biol. 2011; 43:1122–1133. [PubMed: 21514399]

[56]. Xiao H, Zhang YY. Understanding the role of transforming growth factor-beta signalling in the heart: overview of studies using genetic mouse models. Clin Exp Pharmacol Physiol. 2008; 35:335–341. [PubMed: 18290874]

[57]. Copple BL, Bai S, Burgoon LD, Moon JO. Hypoxia-inducible factor-1alpha regulates the expression of genes in hypoxic hepatic stellate cells important for collagen deposition and angiogenesis. Liver international : official journal of the International Association for the Study of the Liver. 2011; 31:230–244. [PubMed: 20880076]

[58]. Li Q, Ren J. Cardiac overexpression of metallothionein attenuates chronic alcohol intake-induced cardiomyocyte contractile dysfunction. Cardiovasc Toxicol. 2006; 6:173–182. [PubMed: 17347528]

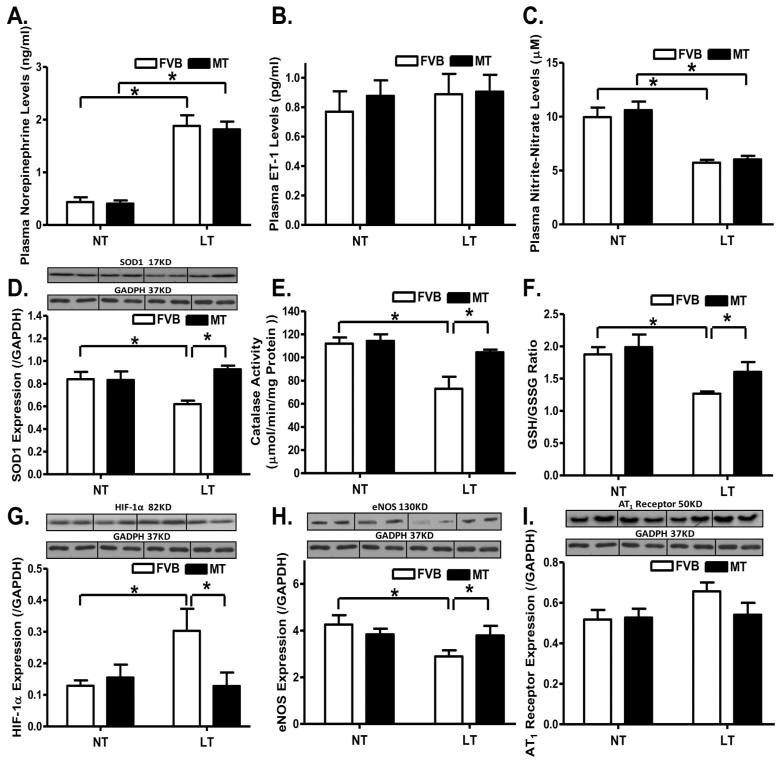

Fig. 1.

Effect of heavy metal scavenger metallothionein (MT) on low temperature (LT, 4°C, 3 months)-induced changes in plasma levels of norepinephrine, ET-1 and nitric oxide, antioxidant capacity, expression of HIF-1α, eNOS and AT_1 receptor. FVB and MT mice were kept at room temperature or 4°C for 3 months. A: Plasma norepinephrine; B: Plasma ET-1 levels; C: Plasma NO levels; D: SOD1 expression; E: Catalase activity; F: GSH/GSSG ratio; G: HIF-1α expression; H: eNOS expression; and I: AT_1 receptor expression. NT: normal temperature, Mean ± SEM, n = 8–9 mice per group, * $p < 0.05$.

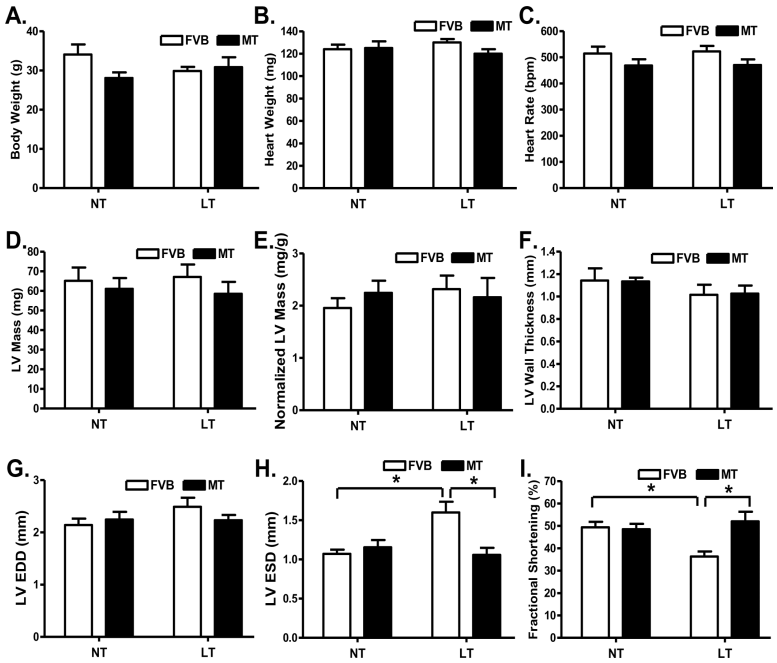

Fig. 2.

Effect of heavy metal scavenger metallothionein (MT) on low temperature (LT, 4°C, 3 months)-induced echocardiographic alterations. FVB and MT mice were kept at room temperature or 4°C for 3 months prior to echocardiographic assessment. A: Body weight; B: Heart weight; C: Heart rate; D: Left ventricular mass; E: Normalized LV mass (to body weight); F: LV wall thickness; G: LV end diastolic diameter (EDD); H: LV end systolic diameter (ESD); and I: Fractional shortening. NT: normal temperature, Mean ± SEM, n = 11 mice per group, * $p < 0.05$.

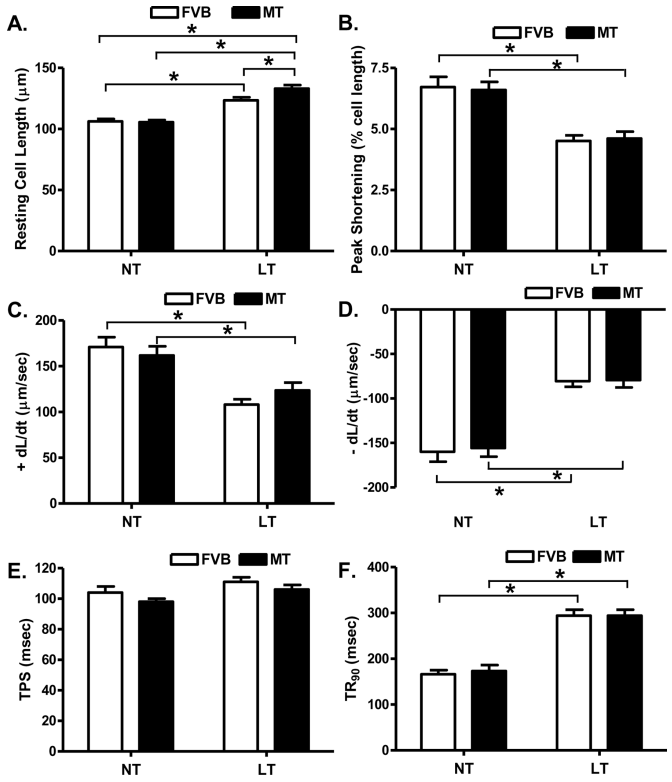

Fig. 3.

Effect of heavy metal scavenger metallothionein (MT) on low temperature-induced cardiomyocyte contractile dysfunction. FVB and MT mice were kept at room temperature or 4°C for 3 months prior to the mechanical assessment. A: Resting cell length; B: Peak shortening (PS, normalized to cell length); C: Maximal velocity of shortening (+ dL/dt); D: Maximal of relengthening (− dL/dt); E: Time-to-PS (TPS) and F: Time-to-90% relengthening (TR_{90}). Mean ± SEM, n = 123 –126 cells from 4 mice per group, * $p < 0.05$, NT: normal temperature.

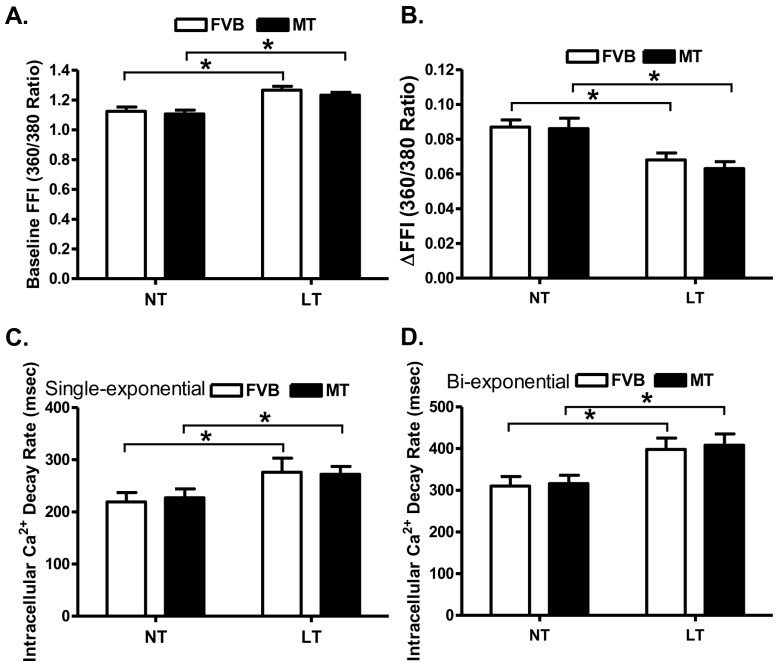

Fig. 4.

Effect of heavy metal scavenger metallothionein (MT) on low temperature (LT, 4°C, 3 months)-induced change in intracellular Ca^{2+} homeostasis in cardiomyocytes. FVB and MT mice were kept at room temperature or 4°C for 3 months prior to intracellular Ca^{2+} assessment. A: Resting fura-2 fluorescence intensity (FFI); B: Electrically-stimulated rise in FFI (ΔFFI); C: Single exponential intracellular Ca^{2+} decay rate; and D: Bi exponential intracellular Ca^{2+} decay rate. Mean ± SEM, n = 59 – 60 cells from 4 mice per group, * $p < 0.05$, NT: normal temperature.

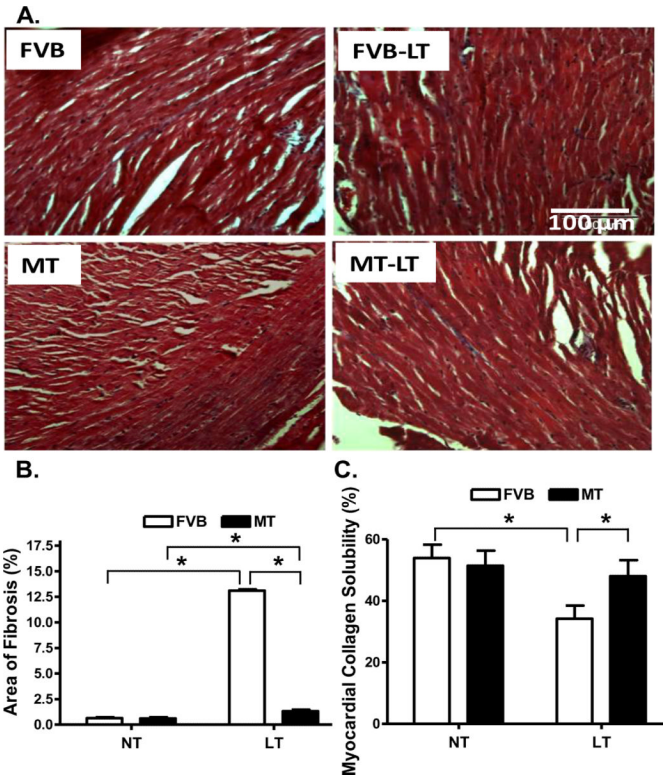

Fig. 5.

Histological analyses of myocardial fibrosis in FVB and metallothionein (MT) transgenic mice maintained at low temperature (LT, 4°C) for 3 months. A: Representative Masson Trichrome staining micrographs showing longitudinal sections of left ventricular myocardium (× 200); B: Quantitative analysis of fibrotic area (Masson trichrome stained area in light blue color normalized to the total myocardial area) from ~ 100 sections from 4 mice per group; and C: Myocardial collagen crosslinking from 6 mouse hearts per group. Mean ± SEM, * $p < 0.05$, NT: normal temperature.

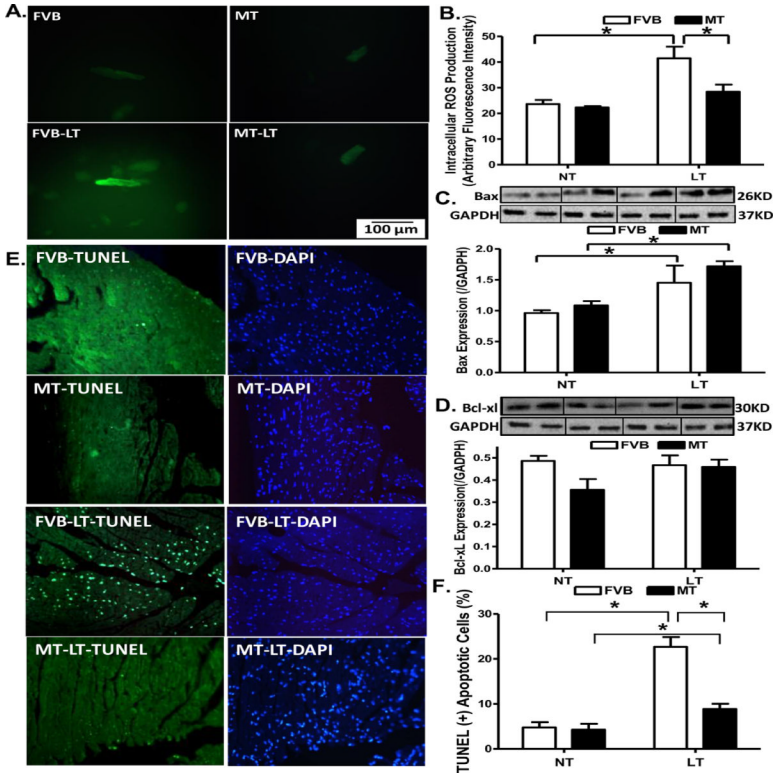

Fig. 6.

Effect of metallothionein (MT) on ROS production and apoptosis in mice maintained at low temperature (LT, 4°C) for 3 months. A: Representative DCF fluorescent images (400×) showing ROS production in cardiomyocytes from FVB and MT mice with or without low temperature exposure; B: Pooled data of ROS production from 15 fields from 4 mice per group; C: Bax expression; and D: Bcl-xl expression. Insets: Representative gels depicting Bax and Bcl-xl expression using specific antibodies. GAPDH was used as the loading control; D: Assessment of apoptosis using TUNEL staining in myocardium. All nuclei were stained with DAPI shown in blue in the right column. The TUNEL-positive nuclei were visualized with fluorescein (green) in the left column. Original magnification = 400×. Quantified data are shown in panel F. Mean ± SEM, n = 3–5 mice (panels C–D) or 12 fields from 3 mice (panel F) per group, * $p < 0.05$, NT: normal temperature.

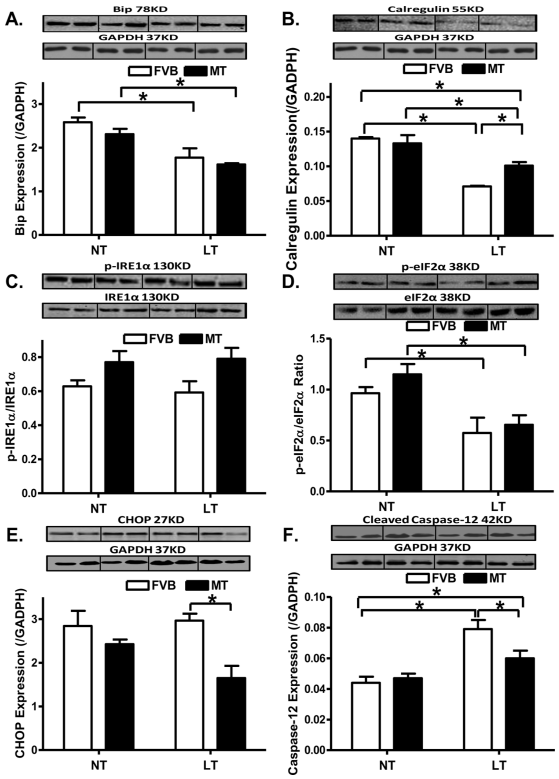

Fig. 7.

Effect of metallothionein (MT) on low temperature (LT, 4°C, 3 months)-induced change in ER stress markers and ER stress-related apoptosis. A: Bip expression; B: Calregulin expression; C: IRE1α phosphorylation (normalized to total IRE1α); D: eIF2α phosphorylation (normalized to total eIF2α); E: CHOP expression; and F: Cleaved caspase-12 expression. Insets: Representative gels depicting ER stress markers using specific antibodies. GAPDH was used as the loading control. Mean ± SEM, n = 3 – 5 mice per group, * $p < 0.05$, NT: normal temperature.

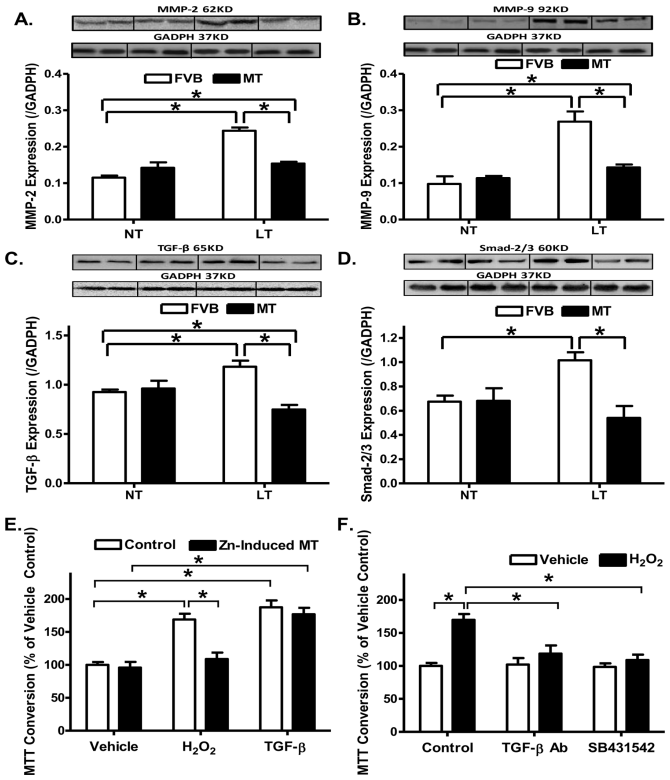

Fig. 8.

Effect of metallothionein (MT) on low temperature (LT, 4°C, 3 months)-induced change in the expression of MMP-2, MMP-9, TGF-β and Smad-2/3 as well as TGF-β-stimulated cell growth in fibroblasts using 3-(4,5-dimethylthiazol-2-yl)-2,5-diphenyltetrazolium bromide (MTT) assay. Metallothionein (MT) was induced using Zinc (50 μM for 24 hrs). For MTT assay, cardiac fibroblasts were treated with TGF-β (2 ng/ml) or positive control H_2O_2 (50 μM) for 24 hrs and cell numbers were normalized to the respective vehicle control group. A: MMP-2 expression; B: MMP-9 expression; C: TGF-β expression; D: Smad-2/3 expression. Insets: Representative gels depicting myocardial MMP-2, MMP-9, TGF-β and Smad-2/3 using specific antibodies. GAPDH was used as the loading control. E: Effect of MT on H_2O_2- and TGF-β-induced cardiac fibroblast cell growth using MTT assay; and F: Effect of TGF-β neutralizing antibody (0.1 μg/ml) and Smad-2/3 blocker SB431542 (10 μM) on H_2O_2-induced cardiac fibroblast cell growth. Mean ± SEM, n = 4 – 6 mice or cultures per group, * $p < 0.05$, NT: normal temperature.

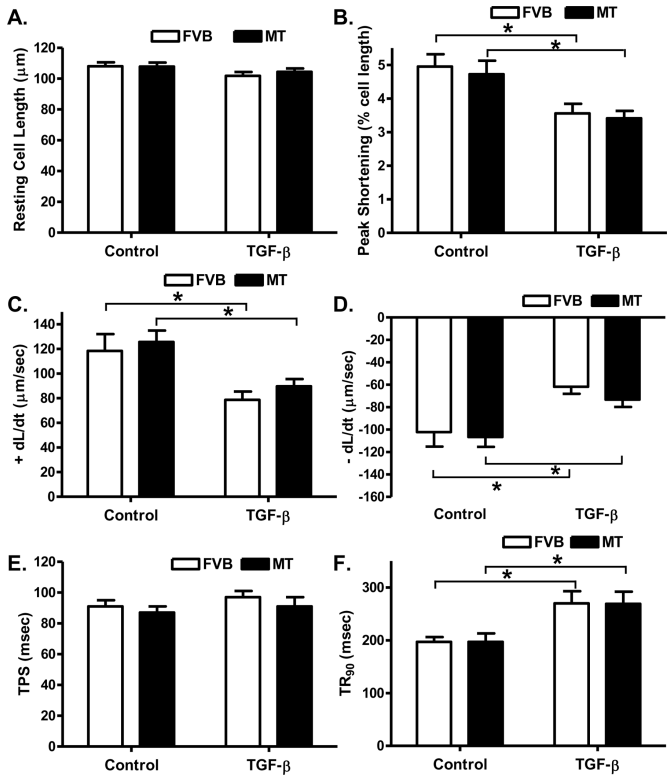

Fig. 9.

Effect of TGF-β on cardiomyocyte contractile function in myocytes isolated from FVB and metallothionein (MT) mice (maintained at normal temperature). A: Resting cell length; B: Peak shortening (PS, normalized to cell length); C: Maximal velocity of shortening (+ dL/dt); D: Maximal of relengthening (− dL/dt); E: Time-to-PS (TPS) and F: Time-to-90% relengthening (TR_{90}). Mean ± SEM, n = 73 – 80 cells from 3 mice per group, * $p < 0.05$.